

# Diffusion and vibrational relaxation of a diatomic molecule in the pore network of a pure silica zeolite: A molecular dynamics study

Pierfranco Demontis, Giuseppe B. Suffritti, and Antonio Tilocca  
*Dipartimento di Chimica, Università degli Studi di Sassari, Via Vienna 2, I-07100 Sassari, Italy*

(Received 21 November 1995; accepted 21 June 1996)

The vibrational relaxation and the diffusion of diatomic molecules in the zeolite silicalite have been studied through molecular dynamics simulations in the microcanonical statistical ensemble. The adopted model accounts for the vibrations of the framework and sorbed atoms using a harmonic potential for the silicalite and a Morse potential for the diatomic molecule. The results show that the framework favors the relaxation of diatomics oscillating at frequencies near to its characteristic vibrational frequencies, leading in such cases to lower relaxation times and to an increasing in the energy exchanged *per collision*. The diffusion of a two-site oscillating molecule representing ethane has been also investigated; the diffusion coefficient and the heat of adsorption agree very well with the experimental data. Arrhenius parameters for the diffusion have been calculated, and some insights into the diffusion mechanism have been obtained from log–log plots and by inspection of the distribution of the ethane molecules in the silicalite channels. Therefore the simplified model adopted seems to adequately describe the diffusive motion and the guest–host energy exchanges, and it could be useful in order to study simple bimolecular reactions in zeolites. © 1996 American Institute of Physics. [S0021-9606(96)51436-4]

## INTRODUCTION

Zeolites are crystalline microporous aluminosilicates, with internal cavities and channels of molecular dimensions; this peculiarity leads to a large number of applications in catalytic and separation process. The knowledge of the properties of the sorbed molecules in a specific zeolite is essential for the understanding and the optimization of such processes. Geometric effects like pore size and pore shape along with interconnectivity and tortuosity are among the relevant parameters necessary to account for diffusion and energy transfer in confined regions. In recent years computer simulations provided a powerful and versatile tool of exploring the behavior of guest molecules in zeolites.<sup>1</sup> Molecular dynamics<sup>2,3</sup> (MD) experiments produce a detailed description of the time evolution of the simulated system, giving access to both structural and dynamic (time-dependent) properties.

In most MD studies the zeolite framework is considered to be rigid, i.e., the atoms are held fixed in their equilibrium positions. This assumption reduces the number of interactions to evaluate in the force loop of the MD computer code, then leading to a decrease in computer time, but, among the others, has a shortcoming; the sorbates diffuse in a static environment without the possibility of exchanging energy with the zeolite framework. Simulations with a vibrating lattice showed that the framework can act as an effective “heat bath” for the sorbates; at any time their velocities are thermalized to a Boltzmann distribution through a continuous energy exchange with the lattice atoms.<sup>4</sup> This fact can have some effects on the diffusion and other properties of the guest species; until now MD studies on this topic have mainly concerned with adsorbed Lennard-Jones (LJ) spheres, representing methane or xenon.<sup>4–9</sup> The effects of framework vibrations should be greater on nonspherical sorbates larger than methane. These species move in a potential with higher

energy barriers to diffusion compared to methane, and the framework vibrations, which can lower these barriers, could have more important effects. In the present paper we study the diffusion of ethane in silicalite; ethane is modeled by two bonded LJ sites, where the bond is represented by a Morse potential function, and framework vibrations are reproduced by a three-dimensional network of harmonic springs which connect nearest neighbors. We will show that this simplified model can well reproduce the main experimental properties of ethane in silicalite, also providing some informations about the diffusion mechanism.

The guest–host energy exchanges can also have important effects in catalytic process, e.g., in the thermal activation of reagents and in the stabilization of excited reaction products. Our interest is in the latter case; we investigate the vibrational relaxation of a diatomic oscillator in the silicalite host, changing its frequency in the range 180–1050 cm<sup>-1</sup>, i.e., the range covered by the IR bands of silicalite which are reproduced by our model. In this way we will show the existence and the extent of coupling effects between the internal vibrations of the diatomic and the silicalite modes.

## THE MODEL

Silicalite is the dealuminated form of synthetic zeolite ZSM-5; simulations are often carried out on silicalite because it is isostructural with ZSM-5, but contains no charge-balancing ions; therefore the long-range Coulombic interactions are absent, and the calculations are simplified. We represented silicalite crystal structure, according to x-ray diffractions studies,<sup>10</sup> in the Pnma space group (orthorhombic), with unit cell lattice parameters  $a=20.022$  Å,  $b=19.899$  Å,  $c=13.383$  Å. The silicalite structure is characterized by two types of channels, see Fig. 1, whose kinetic diameter is about

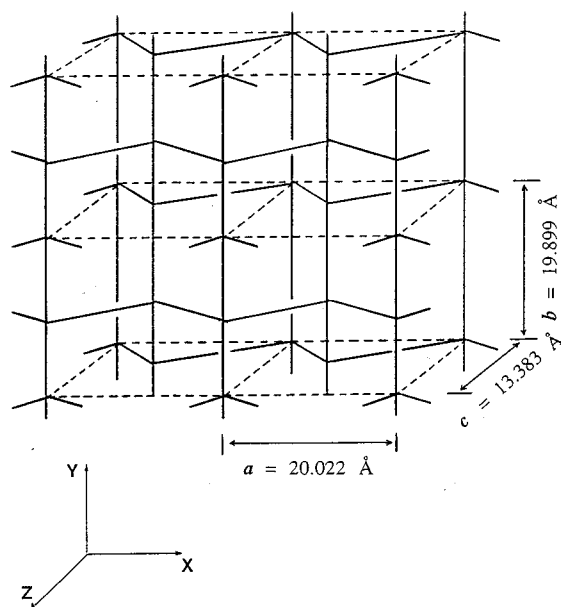


FIG. 1. A schematic representation of the pore network of silicalite. The straight and sinusoidal channel systems are directed along the  $y$  and  $x$  directions, respectively.

5.5 Å; the straight channels run parallel to the  $b$  direction, and the average direction of the sinusoidal channels is  $a$ .

For MD simulations, the simulation box consisted of two crystallographic cells superimposed along  $c$ , resulting in 576 framework atoms (192 Si and 384 O); periodic boundary conditions were applied. Simulations were carried out in the microcanonical (NVE) ensemble; the time step was 1 fs, leading to energy fluctuations lower than 0.1%. The equations of motion were integrated using a modified version of the Verlet algorithm.<sup>11</sup> The harmonic model for the silicalite framework is described in detail in Refs. 12 and 13; only interactions between first neighbors Si–O and O–O are accounted for, through quadratic functions of the displacement from a given equilibrium distance. No other contacts are included and the initial topology of the framework bonds is retained during the MD simulation. This model satisfactorily reproduces the main structural and dynamical features of silicalite, natrolite and zeolite A; the simulated IR spectrum agrees fairly well with the experimental bands, so that framework vibrations are well represented.<sup>14</sup> Ethane and the diatomic molecules used in the simulations are modeled by two LJ interaction sites; the intramolecular potential is of the Morse form

$$U(r) = D[1 - e^{-\beta(r-r_0)}]^2, \quad (1)$$

where

$$\beta = \sqrt{\frac{\mu}{2D}} \omega; \quad \omega = 2\pi c\tilde{\nu}.$$

$\mu$  is the reduced mass; the bond energy and the equilibrium bond length are 351.381 kJ mol<sup>-1</sup> and 1.536 Å, obtained from spectroscopic data for ethane; the mass of each site is 15.024 amu, i.e., the mass of a methyl group; for the diatom-

ics we change the bond frequency by changing  $\beta$ ; for ethane  $\beta$  is fixed to 1.8408 Å<sup>-1</sup>, corresponding to its C–C stretching frequency of 945 cm<sup>-1</sup>.

The Lennard-Jones (12-6) potential is used to describe both the site to site interactions and the site to framework oxygens interactions; as in the most of the MD simulations, we assume that the Si atoms are well shielded by the larger oxygen atoms, so that their interactions with the host species are not accounted for directly. We adopted the site to site LJ parameters obtained by Jorgensen *et al.*<sup>15</sup> for liquid ethane;  $\sigma = 3.775$  Å and  $\epsilon = 0.867$  kJ mol<sup>-1</sup>. The site-to-oxygen LJ parameters are  $\sigma = 3.461$  Å and  $\epsilon = 0.811$  kJ mol<sup>-1</sup>, which, in previous simulations,<sup>4</sup> provided an adequate description of methane–silicalite interaction, and are consequently fairly suitable for describing (CH<sub>3</sub>)–O interactions.

## ETHANE DIFFUSION

Simulations were carried out with eight ethane molecules, which were initially arranged in the sinusoidal and straight channels. The system was thermalized, by scaling the atoms velocities, for 400 ps. This long equilibration time was due to the slow thermalization of ethane molecules. After that, the “production run” was started; we found that very long trajectory (3 ns) were needed in order to achieve a good statistical description of the diffusive process. The center of mass coordinates and velocities of ethane molecules were stored every 32 fs.

A first test of the model used was the calculation of the heat of adsorption, defined as

$$H = \langle U_{gh} \rangle + \langle U_{gg} \rangle - RT, \quad (2)$$

where  $\langle U_{gh} \rangle$  is the average ethane–framework interaction energy,  $\langle U_{gg} \rangle$  is the average ethane–ethane interaction energy, and  $R$  is the gas constant. At 303 K we obtained  $H = -30.5$  kJ mol<sup>-1</sup>, in good agreement with the experimental data at 300 K, which converge to a value<sup>16</sup> of  $-31$  kJ mol<sup>-1</sup>.

Figure 2 illustrates the time evolution of the mean square displacement (MSD) at 303 K, as defined by

$$\Delta r^2(t) = \frac{1}{N_0 N} \sum_{t_0=1}^{N_0} \sum_{l=1}^N |\mathbf{r}_i(t_0+t) - \mathbf{r}_i(t_0)|^2, \quad (3)$$

where the  $\mathbf{r}_i$ 's are the center-of-mass coordinates of ethane molecules, and the average is over  $N$  molecules and  $N_0$  time origins. The channel structure of silicalite leads to the anisotropy of the diffusion process; ethane diffuse roughly twice as fast in the  $y$  direction as in the  $x$  direction, while the motion in the  $z$  direction is almost negligible; there are not channels pointing towards  $z$ , and ethane can diffuse in this direction only covering alternate segments of straight and sinusoidal channels, which seldom happens. This is evident from Fig. 2, in which the total MSD and his components are plotted.

Two other simulations at 403 K and 495 K were carried out; the resulting total MSD's are collected in Fig. 3.

We used the Einstein equation in order to obtain diffusion coefficients from the slope of the MSD curves

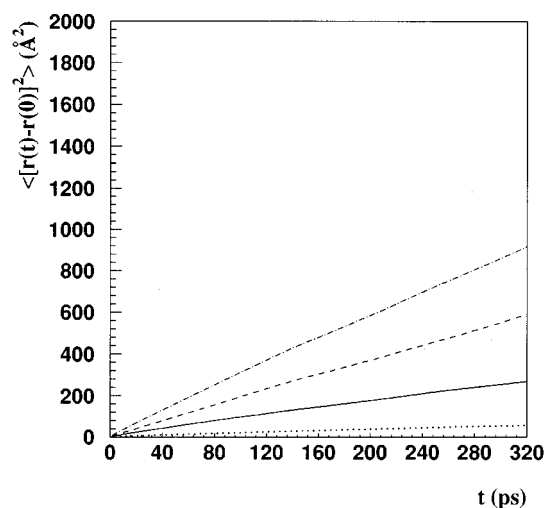


FIG. 2. Mean square displacement for ethane in silicalite at 303 K; total (—), and components  $y$  (---),  $x$  (- - -), and  $z$  (···).

$$D = \lim_{t \rightarrow \infty} \frac{\Delta r^2(t)}{6t}. \quad (4)$$

In Table I the calculated values, obtained with a linear fitting of the curves in the region between 80 and 240 ps are shown. The calculated value of  $D$  at 303 K is  $4.55 \times 10^{-9} \text{ m}^2 \text{ s}^{-1}$ , in good agreement with the experimental value at the same temperature and at the same loading of ethane, which is about  $4 \times 10^{-9} \text{ m}^2 \text{ s}^{-1}$ . The Arrhenius plot (Fig. 4) shows that ethane diffusion is an activated process, i.e., it follows the Arrhenius equation,

$$D = D_0 \exp(-E_a/RT), \quad (5)$$

where  $D_0$  is called the preexponential factor,  $E_a$  is the activation energy,  $R$  is the gas constant, and  $T$  is the temperature. The obtained activation energies and pre-exponential factors are reported in Table II. The highest diffusion coef-

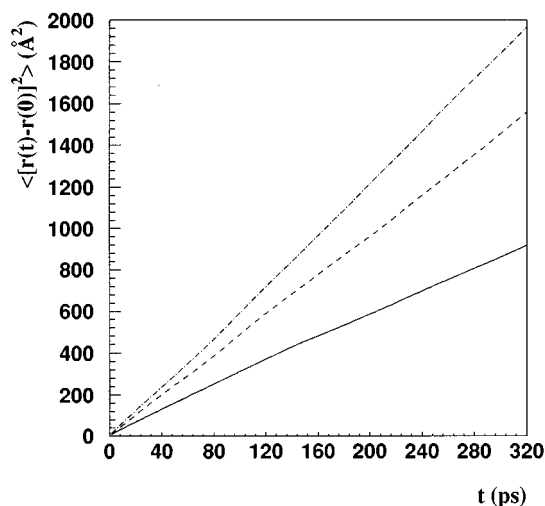


FIG. 3. Total mean square displacement for ethane in silicalite at 303 K (—), 403 K (---) and 495 K (- - -).

TABLE I. Ethane diffusion coefficients.

$T$ (K)	$D/10^{-9}$ ( $\text{m}^2 \text{ s}^{-1}$ )	$D_x/10^{-9}$ ( $\text{m}^2 \text{ s}^{-1}$ )	$D_y/10^{-9}$ ( $\text{m}^2 \text{ s}^{-1}$ )	$D_z/10^{-9}$ ( $\text{m}^2 \text{ s}^{-1}$ )
303	4.5	4.0	8.8	0.8
403	7.9	7.3	15.	1.5
495	10.4	10.7	18.7	1.8

ficient along  $y$  is therefore due both to an higher pre-exponential factor and to a lower activation energy than in the other directions; the  $E_a$ 's along  $y$  and  $z$  are rather similar, and the very slow diffusion along  $z$  is essentially due to the small pre-exponential factor. The Einstein equation is valid on a long time scale only; in order to obtain informations about the diffusive motion at short times, logarithmic plots of MSD turn out to be very helpful.<sup>18</sup> Plotting on logarithmic scale both  $\log(\text{MSD})$  and  $\log(t)$ , every linear region of the resulting plot denotes a distinct diffusive regime, represented by a power law like  $y = Ax^\alpha$ ; e.g., the Einstein diffusive regime is described by a straight line of slope 1. Then it is possible to obtain the characteristic time and space length of every regime, and to draw some conclusion about the diffusion mechanism. In Fig. 5 the logarithmic plot at 303 K is reported; there are clearly three distinct regimes; from 0 to about 0.2 ps, the straight line has slope 2, corresponding to Newtonian dynamics  $R = vt$ ; above 5 ps, the straight line has slope 1, corresponding to the Einsteinian regime  $R^2 = 6Dt$ . Between the two zones, the curve is not linear, representing the transition (changing the slope from 2 to 1) to the Einsteinian regime. The first regime could be identified with a "quasifree" motion of the molecule, which moves in the almost constant potential at the bottom of the adsorption well; this motion is interrupted by the collisions with the channel walls, or with the other molecules. This is evidenced by the center of mass velocity autocorrelation function (Fig. 6) which becomes negative after about 0.2 ps, showing that, on average, every molecule reverse its direction of motion

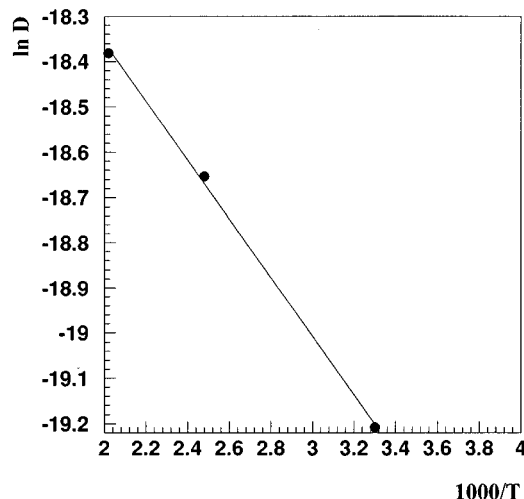


FIG. 4. Arrhenius plot for ethane in silicalite.

TABLE II. Arrhenius pre-exponential factors and activation energies for ethane diffusion in silicalite.

	$D_0/10^{-9}$ ( $\text{m}^2 \text{s}^{-1}$ )	$E_a$ ( $\text{kJ mol}^{-1}$ )
tot	39	5.4
x	48.6	6.3
y	63.8	5.0
z	6.5	5.1

after that time. The average distance covered by the molecule in the transition regime is about 5 Å; after that, the Einstein diffusion occurs. In order to further understand the diffusive mechanisms, the distribution function of ethane molecules in the silicalite channels was calculated; through inverse translation operations the stored coordinates were reported in the unitary cell; this cell was divided in  $40 \times 40 \times 27$  small cubes (side=0.500 55 Å), and we calculated how many configurations placed the center-of-mass of an ethane molecule in each cube. Figure 7 shows the projection of such distribution in the  $yz$  plane, at  $x=0$ , representing the straight channel; the expanded regions at about  $y=5$  and  $y=15$  are the intersections with the sinusoidal channels. The molecules spend most of the time in the regions near the middle of the channels, which appear to be the preferred adsorption sites, and some time near the channel intersections. This finding was already evidenced by June *et al.* using Monte Carlo calculations.<sup>19</sup> According to the “random walk” model, we attempted to describe the diffusive motion of ethane in silicalite as a sequence of activated jumps between these sites. Caro *et al.*<sup>17</sup> obtained a value of about 10 Å using the relation

$$D = l^2/6\tau \quad (6)$$

between the diffusion coefficient  $D$ , the jump length  $l$ , and the mean residence time  $\tau$ . This value is of the order of the

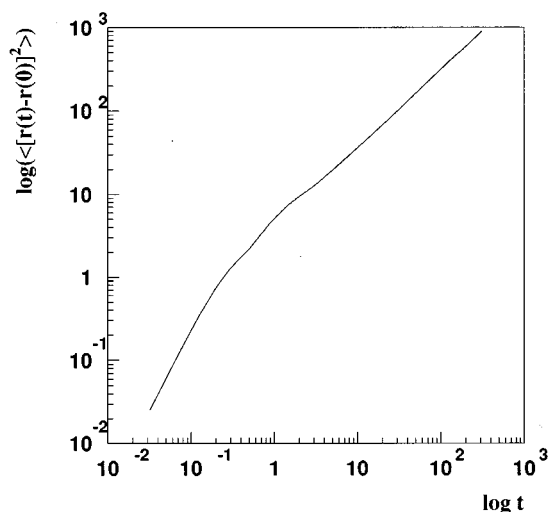
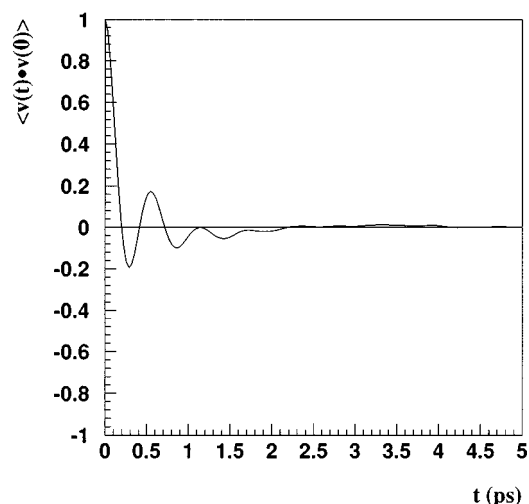
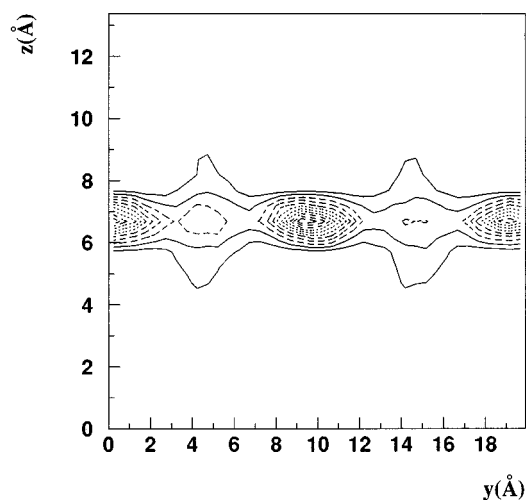
FIG. 5.  $\log_{10}$ - $\log_{10}$  plot of mean square displacement vs time (logarithmic scale) for ethane in silicalite at 303 K.

FIG. 6. Center-of-mass velocity autocorrelation function for ethane in silicalite at 303 K.

distances between adjacent channel intersections so in the above proposed model a molecule jumps between adjacent channel intersections.

If we use the same relation in order to calculate  $\tau$  (with  $D = 4.55 \times 10^{-9} \text{ m}^2 \text{ s}^{-1}$  and  $l = 10 \text{ Å}$ ), we obtain a mean residence time of 36.6 ps, corresponding to an effective jump frequency of  $2.73 \times 10^{10} \text{ s}^{-1}$  at 300 K. However, following the results of our simulations, the jumps should occur between the preferred positions, which are located near the middle of the channels, while the channel intersections switch the trajectories of the molecules to a channel or another in a nearly random way. In conclusion our data show a much more complex diffusive behavior from the one assumed by the jump diffusion model. We therefore tentatively divide the diffusive process in three stages corresponding to three different time scales:

FIG. 7. Center-of-mass distribution function in the  $yz$  plane at  $x=0$ , for ethane in silicalite at 303 K.

- (i) The molecule moves freely for a very short time in the center of channel;
- (ii) The molecule oscillates around a site before jumping to a closer intersection;
- (iii) The Einstein diffusive regime begins after about 5 ps, consisting in activated jumps of length about 5 Å between the favored adsorption sites in the middle of the channels and the channel intersections.

In a recent paper, Dumont *et al.*,<sup>20</sup> studied the same topic with a rigid framework model accounting for the full flexibility and geometry of ethane. They obtained a diffusion coefficient of  $5.9 \times 10^{-9} \text{ m}^2 \text{ s}^{-1}$  for the same conditions as ours; their larger difference from experimental value could be due to the short trajectory carried out (42 ps), which leads to worse statistics, but the effect of the vibrating framework on the diffusive motion of ethane could also be important.

### VIBRATIONAL RELAXATION

Relaxation and diffusion of excited molecules in restricted geometries has been the subject of a variety of experimental and theoretical studies.<sup>21</sup> Simple models have been proposed in order to explain the rich phenomenology indicated by the experimental observations. They attempt to capture the basic geometrical and chemical characteristic of the studied systems by using an idealized representation of pores. In this paper our goal will be to apply a numerical simulation technique in the realm of materials largely used in the industrial plants. The dynamics of the reaction in condensed phases is strongly influenced by the interactions between the reacting system (reagents and products) and the solvent, which can act on the relative diffusion and on the thermal activation of the reactive species, on the overcoming (and the recrossing) of the activation barrier, and on the stabilization of excited products. Some previous MD simulations<sup>22,23</sup> have been directed to examine the role played by the solvent in simple reactions, while in other cases the vibrational relaxation of excited species<sup>24,25</sup> has been taken into account. We studied the vibrational relaxation of one diatomic molecule in the silicalite; this specie does not represent any real molecule, but it can be regarded as a “probe” inserted in the silicalite cavities in order to obtain informations about energy exchanges and coupling effects between the framework and an oscillator of variable frequency. The method followed for bringing the oscillator in a vibrationally excited state is a modification of that used by Ohmine,<sup>25</sup> and is illustrated in Fig. 8. In the equilibration run the intramolecular potential of the sorbed molecule was harmonic

$$U(r) = 1/2k(r - r_{\text{eq}})^2, \quad (7)$$

where the force constant  $k$  was  $2700 \text{ kJ mol}^{-1} \text{ \AA}^{-2}$  corresponding to the force constant of a C–C bond.<sup>26</sup> The equilibration run (at  $T=290 \text{ K}$ ) lasted 75 ps; we applied a double scaling of the velocities at each step; the first on each atom, the second on the molecule only. This turned out to be necessary because it was very difficult to thermalize the molecule only through the first scaling, which depends on the

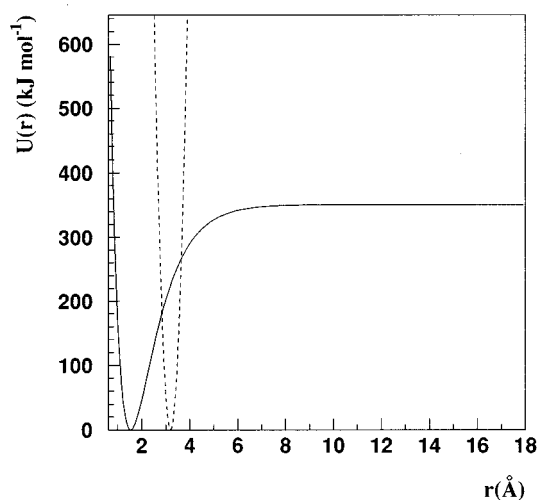


FIG. 8. Harmonic to Morse potential transition; dotted line represents the harmonic potential used in the equilibration run; continuous line represents the Morse potential.

overall kinetic temperature, and so it is inefficient for the single molecule. Once the equilibrium was reached, we changed the harmonic potential to the Morse form, with a  $\beta$  value depending on the frequency chosen, without changing the positions and the velocities of the two oscillating masses. This correspond to a sort of vertical transition which gives rise to a vibrational excitation, whose extent depends on the  $r_{\text{eq}}$  value, i.e., on the position of the “harmonic” curve compared to the “Morse” curve (which is centered at  $r_0=1.536 \text{ \AA}$ ). In this way the rotational and translational energies of the molecule maintain the values reached after the equilibration run. In order to compare the results at different frequencies, in each simulation run we adjusted the  $r_{\text{eq}}$  value so, when the transition happened, the “excitation” potential energy would be always about  $230 \text{ kJ mol}^{-1}$ . This is a high value, but well

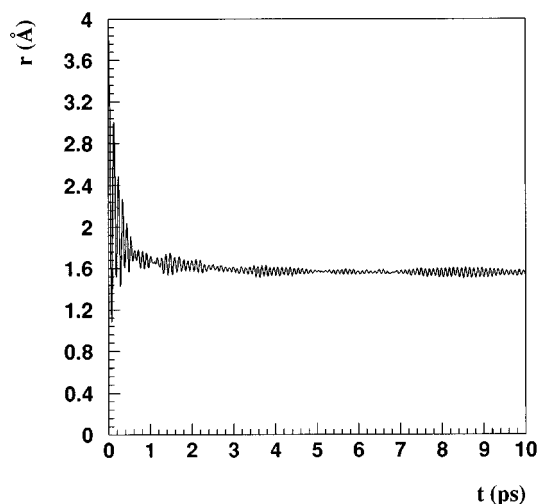


FIG. 9. Evolution of the bond length in the first 10 ps for the  $341 \text{ cm}^{-1}$  oscillator (averaged over 40 trajectories).

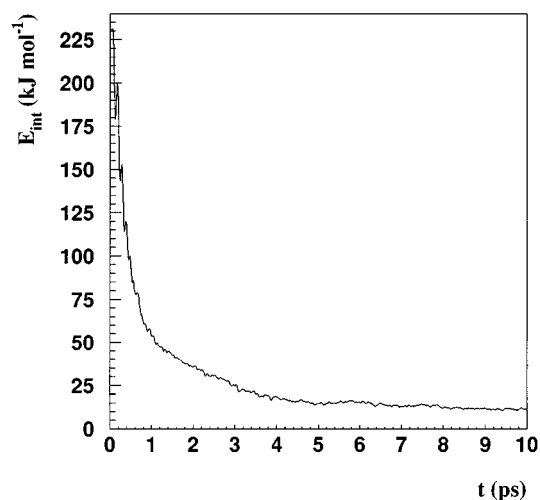


FIG. 10. Evolution of the internal energy in the first 10 ps for the  $341\text{ cm}^{-1}$  oscillator (averaged over 40 trajectories).

below the dissociation limit ( $\sim 350\text{ kJ mol}^{-1}$ , as stated before). After that, the relaxation of the oscillator was followed, observing the time evolution of some properties, like the bond length (Fig. 9). We examined 11 different frequencies; for each frequency, we carried out 40 simulations starting with different initial conditions, and we averaged the obtained results. One obtains different initial conditions by switching on the transition at different times after the end of the equilibration run; in this view, the method followed has the advantage of providing these “excited” initial conditions in a simple and equilibrated manner, because with this kind of transition we do not change the bond length neither the velocities.

The oscillator internal energy, i.e., the sum of the kinetic and the Morse potential energy, turns out to be the best property to follow in order to estimate the relaxation rate; it does not oscillate as strongly as the bond length, or the potential energy (Fig. 10), so that fitting operations are easier. It would have been suitable to fit curves like Fig. 10 with exponentials like  $e^{-bt}$ , taking the  $b$  value as estimate of the relaxation rate; but, while at low-frequency the relaxation is fast (e.g., a few picoseconds, like in Fig. 10), increasing the oscillation frequency leads to very long relaxation times (some hundreds of picoseconds for the  $1045\text{ cm}^{-1}$  oscillator). Following the 40 trajectories (for each frequency) for such a long time would have required too much computer time, then we used a different parameter to characterize the relaxation rate, i.e., the *half-relaxation time*,<sup>8</sup> as defined by

$$\Delta E(t_{1/2}) = \frac{1}{2} \Delta E(t=0), \quad (8)$$

where  $\Delta E$  is the difference between the oscillator internal energy and the energy of a generic framework atom. This last value was obtained by averaging the total kinetic energy of Si and O atoms, plus the potential energy O–O and Si–O, over the total number of framework atoms; it rises very slowly, because the framework receives the energy excess of only one sorbed molecule. Through the calculation of the

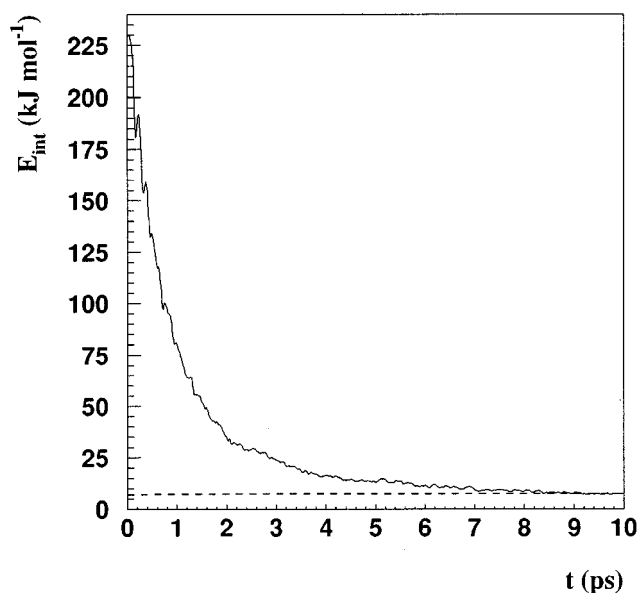


FIG. 11. Internal energies of the oscillator (upper curve) and of the framework (lower curve, averaged over all the Si and O atoms), for the  $227\text{ cm}^{-1}$  oscillator.

half relaxation time one cannot wait for the molecule to reach the equilibrium, and computation times turn to be shortened. In Fig. 11 the above-mentioned internal energies for the  $227\text{ cm}^{-1}$  oscillator are illustrated; the  $t_{1/2}$  value is 0.6 ps. The results are also shown in Table III. Assuming that the relaxation rate decreases exponentially with the frequency (as observed by Holian in Ref. 24), if we plot the natural logarithm of  $t_{1/2}$  vs the wave number, we should obtain a straight line. We can see in Fig. 12 that all the points stay on a straight line, except for the four points from  $341$  to  $614\text{ cm}^{-1}$ . This anomalous behavior can be due to the coupling with the vibrational modes of the framework. Indeed, the IR spectrum of silicalite reproduced by our model<sup>14</sup> shows a large band in that region, corresponding to collective vibrations of Si and O atoms, and, therefore, the relaxation rate of species oscillating in the same frequency range appears to increase. Moreover, it seems that similar effects are absent in the range near  $1000\text{ cm}^{-1}$ , corresponding to the other IR

TABLE III. Half-relaxation times.

Frequency ( $\text{cm}^{-1}$ )	$t_{1/2}$ (ps)
180	0.47
227	0.6
341	0.34
420	0.76
500	2.79
557	2.14
614	9.84
829	62.3
945	124.6
1000	191.2
1045	244.8

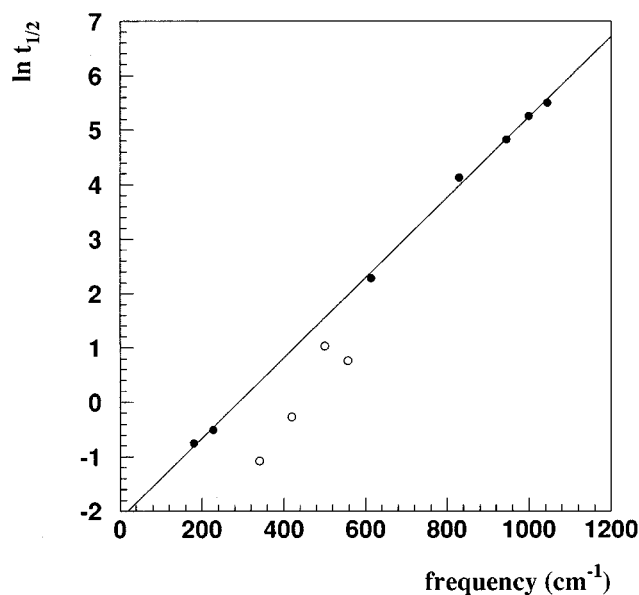


FIG. 12. Logarithm of the half-relaxation time vs wave number; the full circles represents the points that have not been included in the linear fitting.

band (Si–O stretching modes). In order to further examine this topic and to better understand the energy exchange mechanisms, we studied in detail the collisions between the oscillator and the framework. A collision was defined as the situation in which an oscillator site and an oxygen atom comes so close that the interaction potential energy was positive. Then this energy rises up to a maximum  $V_{\max}$  and finally decreases becoming again negative. The duration of the collision is the total time in which the potential energy is positive. We carried out some simulations at different frequencies (the same as before, and also for other values, extending the range to  $1500\text{ cm}^{-1}$ ), evaluating

- (i) the average duration of a collision;
- (ii) the average number of collisions in the first 10 ps after the transition;
- (iii) the average number of collisions with potential peak  $V_{\max} > 16\text{ kJ mol}^{-1}$ , again in the first 10 ps after the transition;
- (iv) the energy lost on average by the oscillator between the beginning of the collision and the potential peak.

We must notice that binary collisions are rare in condensed phase systems; therefore the oscillator is exchanging energy with several oxygen atoms, and we cannot say that the measured energy is the *energy exchanged in a collision*. It is only an average of the total energy lost by the oscillator in the above-mentioned time. The results are shown in Table IV. The average duration of a collision is illustrated in Fig. 13; it decreases in a very regular way with the increasing frequencies, being close to the oscillator period, except for the low frequencies collisions, which are shorter than the correspondent period. At high and intermediate frequencies, an oscillating mass remains at a repulsive distance from an oxygen atom until the restoring force “withdraws” it. At

TABLE IV. Average duration, number, and energy of the collisions.

Frequency ( $\text{cm}^{-1}$ )	Duration (fs) <sup>a</sup>	Total collision number <sup>b</sup>	Collision number with $V_{\max} > 16^b$	Exchanged energy ( $\text{kJ mol}^{-1}$ ) <sup>b</sup>
180	56.4	221.5	4.9	11.7
227	56.1	206.4	4.6	9.0
300	54.6	203.1	5.6	8.4
341	52.9	216.7	5.7	10.8
420	48.6	225.4	5.3	11.4
500	42.3	262.3	5.1	10.5
557	39.5	273.5	4.4	9.8
614	37.4	260.9	3.3	7.8
720	35.1	240.2	1.6	4.8
829	33.3	237.3	1.1	3.8
945	31.5	233.8	0.2	2.2
1000	29.7	245.9	0.3	2.2
1045	29.9	280	0.4	2.6
1136	28.2	282.9	0.25	2.6
1227	27.5	243.1	0.16	1.6
1300	26.9	291.7	0.2	1.6
1400	25.9	272.6	0.13	1.3
1500	24.8	266.8	0.03	1.1

<sup>a</sup>Averaged over all the collisions in a trajectory, and over 40 trajectory lasting 10 ps each.

<sup>b</sup>Averaged over 40 trajectory lasting 10 ps each.

low frequencies, what moves the oscillating mass away from the collision is no longer the internal vibration, but the overall translational motion of the molecule, whose center-of-mass oscillates in the potential well of the adsorption site. The period of this motion is lower than that of low-frequency vibration, and leads to shorter collisions. The total number of collisions does not have a well-defined trend, while much more interesting is the behavior of the exchanged energy in the time between the beginning and the potential peak of a collision; we normalized this energy by dividing it by the corresponding duration, so as to obtain an estimate of energy

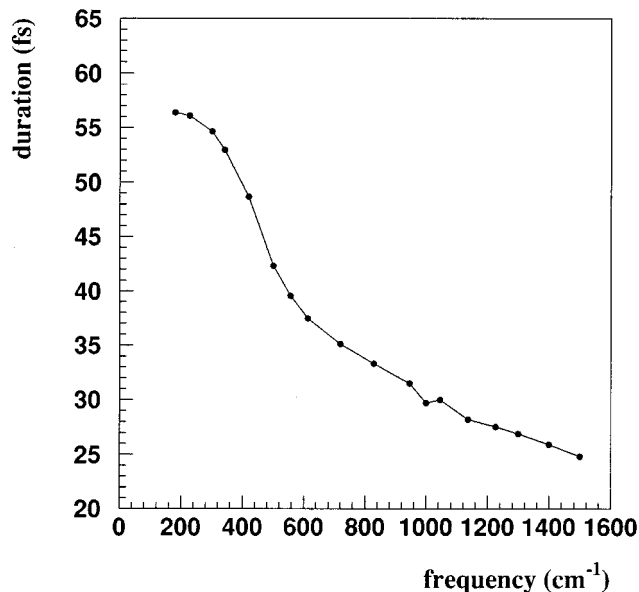


FIG. 13. Average duration of a collision in the first 10 ps after the transition.

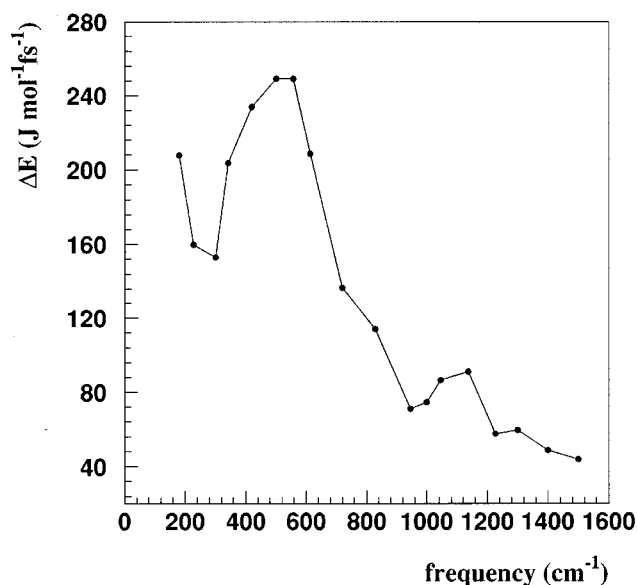


FIG. 14. Energy amount lost by the oscillator per time unit.

exchanged for time unit, at the different frequencies, reported in Fig. 14. There are two peaks, superimposed to the general decrease, which roughly corresponds to the two IR aforementioned bands. These peaks could be due to coupling effects with the vibrational modes; the main coupling is in the range 300–600 cm<sup>-1</sup>, and it is also observable in the lower half-relaxation times; a less evident, but significant, coupling is in the 1000 cm<sup>-1</sup> zone, corresponding to Si–O stretching modes. The framework appears to act in favor of the relaxation of species oscillating at frequencies close to its characteristic frequencies, through an increase in the amount of exchanged energy for the time unit.

Finally, we observed that also the collision number with  $V_{\max} > 16 \text{ kJ mol}^{-1}$  increases in the aforementioned “resonant” frequency ranges; therefore the “strong” collisions, although very rare (from almost 0 to 2% of the total number), could play some role in the observed coupling phenomena.

## CONCLUSIONS

Molecular dynamics simulations using a model which accounts for the framework flexibility and the internal vibrations of the sorbed species, represented by two oscillating Lennard-Jones spheres, provided an accurate description of diffusive motion of ethane in silicalite, reproducing very satisfactorily experimental data, and also giving some detailed informations about the diffusion mechanisms. Arrhenius diffusion parameters have also been obtained. The calculated diffusion coefficient is slightly better than that obtained with a fixed framework model accounting for the full geometry and flexibility of ethane, suggesting that framework flexibility and energy exchanges could play an important role in the diffusion process. The harmonic model of the framework also gave a realistic description of coupling phenomena connected to the energy exchanges with the sorbed species. Silicalite can stabilize vibrationally excited species, extracting from it the energy excess, in a picosecond time scale. We argue that the observed effects will be much more evidenced when increasing the molecular complexity of the adsorbed species because there will exist lower-frequency modes that are more easily excited. We stress that the use of *classical* mechanics for drawing these conclusions and, in general, for studying the dynamics of microscopic systems like the one considered in this paper, where the *quantum* mechanics should be applied, deserve some comments. For translational motion, it is well known that the classical mechanics yields good approximations of the quantum results, as far as energy barriers are low and light atoms (like the hydrogen isotopes) are not involved, and this is true for ethane in silicalite. As free rotations are lacking in the considered system, all other motions have a vibrational or oscillatory character. If they are harmonic, there are simple correspondence rules relating the classical frequencies and amplitudes to the quantum energy levels and amplitudes, respectively. If anharmonic motions are present, some (usually small) corrections should be applied.<sup>27</sup> The transfer of energy from a vibrationally excited molecule is a quantum phenomenon, being more probable when the energy level gaps of the molecule are equal or larger but close to those of the framework. For harmonic oscillators, the energy level gaps are proportional to the frequency, and the quantum energy transfer corresponds to the classical resonance between oscillators, where the maximum energy transfer rate occurs when the frequencies of the oscillators are the same. The dependence of the energy transfer rate on frequency is not so different in quantum and in classical mechanics, so that, even if oscillators in real systems often are not exactly harmonic, from the above considerations it appears reasonable to use classical MD as a guideline for the study of energy transfer phenomena like the ones which are described in this paper. A development of the present work is the study of simple bimolecular reactions in zeolites, which is in progress.

calite can stabilize vibrationally excited species, extracting from it the energy excess, in a picosecond time scale. We argue that the observed effects will be much more evidenced when increasing the molecular complexity of the adsorbed species because there will exist lower-frequency modes that are more easily excited. We stress that the use of *classical* mechanics for drawing these conclusions and, in general, for studying the dynamics of microscopic systems like the one considered in this paper, where the *quantum* mechanics should be applied, deserve some comments. For translational motion, it is well known that the classical mechanics yields good approximations of the quantum results, as far as energy barriers are low and light atoms (like the hydrogen isotopes) are not involved, and this is true for ethane in silicalite. As free rotations are lacking in the considered system, all other motions have a vibrational or oscillatory character. If they are harmonic, there are simple correspondence rules relating the classical frequencies and amplitudes to the quantum energy levels and amplitudes, respectively. If anharmonic motions are present, some (usually small) corrections should be applied.<sup>27</sup> The transfer of energy from a vibrationally excited molecule is a quantum phenomenon, being more probable when the energy level gaps of the molecule are equal or larger but close to those of the framework. For harmonic oscillators, the energy level gaps are proportional to the frequency, and the quantum energy transfer corresponds to the classical resonance between oscillators, where the maximum energy transfer rate occurs when the frequencies of the oscillators are the same. The dependence of the energy transfer rate on frequency is not so different in quantum and in classical mechanics, so that, even if oscillators in real systems often are not exactly harmonic, from the above considerations it appears reasonable to use classical MD as a guideline for the study of energy transfer phenomena like the ones which are described in this paper. A development of the present work is the study of simple bimolecular reactions in zeolites, which is in progress.

## ACKNOWLEDGMENTS

This research is supported by M.U.R.S.T. (60% and 40%) and by Consiglio Nazionale delle Ricerche, Grant No. 20710.3237.93.

<sup>1</sup> *Modeling of Structure and Reactivity in Zeolites*, edited by C. R. A. Catlow (Academic, London, 1992).

<sup>2</sup> *Simulations of Liquids and Solids*, edited by G. Ciccotti, D. Frenkel, and I. R. McDonald (North-Holland, Amsterdam, 1987).

<sup>3</sup> M. P. Allen and D. J. Tildesley, *Computer Simulations of Liquids* (Clarendon, Oxford, 1987).

<sup>4</sup> P. Demontis, G. B. Suffritti, E. S. Fois, and S. Quartieri, *J. Phys. Chem.* **96**, 1482 (1992).

<sup>5</sup> P. Demontis and G. B. Suffritti, *Chem. Phys. Lett.* **223**, 355 (1994).

<sup>6</sup> P. Demontis, E. S. Fois, G. B. Suffritti, and S. Quartieri, *J. Phys. Chem.* **94**, 4329 (1990).

<sup>7</sup> S. Fritzsche, R. Haberlandt, J. Kaerger, H. Pfeifer, and M. Wolfsberg, *Chem. Phys. Lett.* **171**, 109 (1990).

<sup>8</sup> G. Schrimpf, M. Schlenkrich, Jurgen Brickmann, and P. Bopp, *J. Phys. Chem.* **96**, 7404 (1992).

<sup>9</sup> P. Demontis, G. B. Suffritti, and P. Mura, *Chem. Phys. Lett.* **191**, 553 (1992).



- <sup>10</sup>H. van Koningsveld, H. van Bekkum, and J. C. Jansen, *Acta Crystallogr. B* **43**, 127 (1987).
- <sup>11</sup>L. Verlet, *Phys. Rev.* **98**, 159 (1967).
- <sup>12</sup>P. Demontis, G. B. Suffritti, S. Quartieri, E. S. Fois, and A. Gamba, *Zeolites* **7**, 522 (1987).
- <sup>13</sup>P. Demontis, G. B. Suffritti, S. Quartieri, E. S. Fois, and A. Gamba, *J. Phys. Chem.* **92**, 867 (1988).
- <sup>14</sup>P. Demontis, G. B. Suffritti, S. Quartieri, A. Gamba, and E. S. Fois, *J. Chem. Soc. Faraday Trans.* **87**, 1657 (1991).
- <sup>15</sup>W. L. Jorgensen, J. D. Madura, and C. J. Swenson, *J. Am. Chem. Soc.* **106**, 6638 (1984).
- <sup>16</sup>B. Smit, *J. Phys. Chem.* **99**, 5597 (1995), and references therein.
- <sup>17</sup>J. Caro, M. Bulow, W. Schirmer, J. Karger, W. Heink, H. Pfeifer, and S. P. Zdanov, *J. Chem. Soc. Faraday Trans. I* **81**, 2541 (1985).
- <sup>18</sup>S. El Amrani and M. Kolb, *J. Chem. Phys.* **98**, 1509 (1993).
- <sup>19</sup>R. L. June, A. T. Bell, and D. N. Theodorou, *J. Phys. Chem.* **94**, 1508 (1990).
- <sup>20</sup>D. Dumont and D. Bougeard, *Zeolites* **15**, 650 (1995).
- <sup>21</sup>*Molecular Dynamics in Restricted Geometries*, edited by J. Klafter and J. M. Drake (Wiley, New York, 1989).
- <sup>22</sup>J. P. Bergsma, P. M. Edelsten, B. J. Gertner, K. R. Huber, J. R. Reimers, K. R. Wilson, S. M. Wu, and J. T. Hynes, *Chem. Phys. Lett.* **123**, 394 (1986).
- <sup>23</sup>I. Benjamin, B. J. Gertner, N. J. Tang, and K. R. Wilson, *J. Am. Chem. Soc.* **112**, 524 (1990).
- <sup>24</sup>B. L. Holian, *J. Chem. Phys.* **84**, 3138 (1986).
- <sup>25</sup>I. Ohmine, *J. Chem. Phys.* **85**, 3342 (1986).
- <sup>26</sup>G. Herzberg, *Infrared and Raman Spectra of Polyatomic Molecules* (Van Nostrand Reinhold, New York, 1945).
- <sup>27</sup>P. H. Berens and K. R. Wilson, *J. Chem. Phys.* **74**, 4872 (1981).